PLANT SCIENCE TODAY
Vol 12(sp1): 1-10
https://doi.org/10.14719/pst.10180

eISSN 2348-1900

RESEARCH ARTICLE

Integrating optical and SAR data for improved mangrove mapping: Performance analysis of OSCMI versus random forest classifier

Sabarinathan Babu[1], S Pazhanivelan[2*], V Geethalakshmi[3], R Kumaraperumal[1], P Kannan[4] & P C Prabu[2]

[1]Department of Remote Sensing & GIS, Tamil Nadu Agricultural University, Coimbatore 641 003, Tamil Nadu, India
[2]Centre for Water & Geospatial Studies, Tamil Nadu Agricultural University, Coimbatore 641 003, Tamil Nadu, India
[3]Tamil Nadu Agricultural University, Coimbatore 641 003, Tamil Nadu, India
[4]Centre for Agricultural Nanotechnology, Tamil Nadu Agricultural University, Coimbatore 641 003, Tamil Nadu, India

*Correspondence email - pazhanivelans@gmail.com

Received: 22 June 2025; Accepted: 28 July 2025; Available online: Version 1.0: 14 October 2025

Cite this article: Sabarinathan B, Pazhanivelan S, Geethalakshmi V, Kumaraperumal R, Kannan P, Prabu PC. Integrating optical and SAR data for improved mangrove mapping: Performance analysis of OSCMI vs. random forest classifier. Plant Science Today. 2025; 12(sp1): 1-10. https://doi.org/10.14719/pst.10180

Abstract

Mangrove Forest (MF) extents and distributions are fundamental for conservation and restoration efforts. According to previous studies, Landsat and Sentinel-2 imageries are widely used for mangrove area mapping. There are also several vegetation indices from optical data for mangroves used to discriminate mangrove from other vegetation. Still, their performance is not satisfactory, especially due to their presence in the intertidal region. To address this limitation, Sentinel-1A SAR images are integrated with optical datasets for mangrove extent mapping. In this study, we have compared mangrove area obtained from two methods, first one is supervised classification using random forest classifier integrating vegetation indices with Sentinel-2 optical datasets. Another approach is threshold segmentation using combined optical and SAR images, as well as the Combined Mangrove Index (CMCI) with VV polarization. The result shows OSCMI based classification yield best results and outperforms random forest classification by optical data. Mangrove area estimated for the study area by OSCMI classification was 2027 ha with the overall accuracy of 84.7 % and kappa coefficient of 0.66. This shows integrating SAR data for mangrove area extraction improves accuracy.

Keywords: mangrove mapping; OSCMI; random forest; Sentinel-1; Sentinel-2

Introduction

Mangroves are unique communities of salt tolerant woody plants that thrive in the intertidal zones of tropical and subtropical coasts. Mangroves are a critical component of the transitional zones between land and sea, encompassing approximately 14.7 million hectares on a global scale. This area accounts for 14.93 % of the total global coastline, which measures around 2 million kilometres, thus emphasizing the ecological significance of these ecosystems on an international level. Among the world's mangrove cover, Asia accounts for 43.8 % and shows substantial ecological and environmental contributions. In India, the total mangrove cover was 4992 sq. km, of which Tamil Nadu accounts for 45 sq. km (1). Mangroves are the most productive among all other ecosystem, offering significant ecological functions and substantial social and economic benefits. This area is more than just a forest offering fodder for animals, preserving water quality by pollutant filtering, giving habitat to different flora and fauna and is associated with biodiversity conservation. They play a crucial role as carbon sinks by sequestering carbon in both their biomass and sediments. It is estimated that mangrove ecosystems across the globe sequester an average of 1.71 Mg C/ha/year (equivalent to 171 Mg C/sq. km/year) (2). At this global sequestration rate, the mangroves located in Tamil Nadu, encompassing an area of approximately 45 sq. km, possess the potential to sequester 7695 Mg C annually (or roughly 28241 Mg CO_2 equivalent per year) (3). The worldwide degradation of mangrove ecosystems constitutes a pressing environmental concern. In recent decades, MFs have experienced significant decline, primarily due to anthropogenic activities and changes in environmental conditions. Research indicates that the global community has witnessed a loss of approximately 5245 sq. km of mangroves from 1996 to 2020, primarily due to the expansion of aquaculture, natural attrition and land conversion for agricultural purposes. Initiatives aimed at their conservation and sustainable management have intensified; however, the rate of loss, despite a decrease from 0.12 % to 0.07 % annually during the period of 2000-2020, continues to pose a significant challenge. According to ISFR report, in India the mangrove cover increasing at average rate of 1.33 % from 2001 to 2021 (1).

Climate change represents a significant threat to mangrove ecosystems. The elevation of sea levels, alterations in precipitation patterns, increasing temperatures and intensified storm activities have direct repercussions on the vitality and distribution of mangroves. Climatic changes have been shown to impact mangrove populations at regional scales, disrupting their growth patterns and decreasing their survival probabilities (4). The elevation of sea levels, for example, may result in heightened saltwater intrusion, which adversely affects species reliant on freshwater within these ecosystems. Ecologically, the deterioration of mangrove ecosystems results in a diminishment of biodiversity and a decrease in the array of ecosystem services they provide, which include coastal protection, carbon sequestration and sustenance for marine organisms. Mangroves serve as a protective barrier against coastal erosion and storm events; their absence heightens the susceptibility of coastal regions to natural calamities. The fragmentation and degradation of MFs facilitate the release of sequestered carbon dioxide, thereby intensifying the ramifications of climate change (4). Comprehensive knowledge of the distribution and functioning of mangrove ecosystems can be obtained through physical or ground-based research. These techniques do have time and geographical restrictions, though (5). Physical surveys make it challenging to gather data on ecological change over extended time periods and wide geographic areas. The presence of water and tidal impacts in mangrove habitats might make change detection studies particularly difficult (6).

Remote sensing technology has emerged as a crucial tool for monitoring spatiotemporal ecological ecosystem changes of mangroves (5). They make it possible to gather spectral and spatial data from MFs, including inaccessible locations where ground measurements are costly and challenging (7). A previous study has mapped different mangrove species distribution of Pichavaram mangrove ecosystem of Tamil Nadu using hyperspectral data (8). The changing dynamics of mangroves along the coast of Tamil Nadu were assessed by using Landsat imagery (9). Generally, two methods were adopted for mangrove extraction. One is a traditional classification method that requires many training sample sets, which is difficult if attempted for a large area. Another one is indices based threshold segmentation (10). Vegetation indices are faster in extracting target objects on a large scale and provide a better representation of vegetation features than individual bands (11). Historically, most research has relied on optical remote sensing data, particularly medium-resolution multispectral images like those from Landsat (12). However, the presence of mixed pixels in these images can compromise the accuracy of mangrove extraction due to their medium spatial resolution (13). High-resolution images from satellites like Worldview and Quickbird are effective but often limited by cost and data volume. High-resolution remote sensing data, including UAV and satellite imagery, is increasingly being utilized for mangrove studies. Difficulties identified by these studies are that all studies use optical data that is mainly influenced by the atmosphere, there is a need for multi-temporal images of high tide and low tide to find the tidal flow, which is in higher demand (14,15). The ability of the indices for mangrove extraction in various regions needs to be further confirmed because many mangrove indices have only been tested in one or a small number of areas (usually with tall and dense mangroves). However, different types of mangroves (tall and dense forest or low and sparse forest, rich or single tree species) will have significant differences in images. In considering all the above constraints, Synthetic Aperture Radar (SAR) can be used as valuable alternative due to its ability to capture data regardless of weather conditions, except in extreme cases. But using only the SAR data involves much understanding about its imaging mechanism and it requires accurate pre-processing of SAR images because there are problems like inherent speckle noise, overlap, shadow and low signal to noise ratio were introduced while image acquisition. So SAR data can be used as supplement to optical data to increase mangrove area extraction accuracy (10). Combining SAR and optical images can enhance the accuracy of mangrove extraction, addressing some of the limitations associated with using either data source alone (16). Various studies have utilized satellite remote sensing data, including optical images and SAR, to map MFs globally. The introduction of Sentinel-1 SAR images has revolutionized land cover classification in cloud-prone environments, as SAR can penetrate cloud cover and provide year-round data.

Optical and SAR images Combined Mangrove Index (OSCMI) is the first threshold segmentation-based mangrove extraction index using SAR and optical data by (10). In this study, we compared the optical-based mangrove area estimation using random forest with SAR and optical combined mangrove vegetation indices.

Material and Method

Study area

The study area, Muthupet mangroves of Thiruvarur district, is located at the southern end of the Cauvery Delta region of Tamil Nadu, on the Bay of Bengal. Thiruvarur district has highest mangrove cover in Tamil Nadu accounting 12.75 sq. km among total mangrove cover of 44.94 sq. km (1). The study area is a contiguous lagoon where *Avicennia marina* is the predominant species, occupying 95 % of the area, followed by *Acanthus ilicifolius* and *Aegiceras corniculatum* (17). Fig. 1 depicts the overview of the study area.

Datasets used

This study uses both optical and SAR satellite imagery for area extraction and accuracy assessment. Optical data, such as Sentinel-2, which is open-source data and commercial higher-resolution Planet Scope imagery, were used for this study area. Sentinel-1 is an open-source active microwave data also downloaded for the same study area. The details of Sentinel-1, Sentinel-2 and Planet Scope data are given in Table 1. This study made use of Google Earth Engine (GEE), a cloud computing platform that stores collections of satellite images and enables the processing and analysis of massive geographical datasets (18).

Table 1. Details of satellite imagery used in this study

Sensor	Sentinel-1	Sentinel-2	Planet scope
No.of bands	C-band	13 bands	8 bands
Spatial resolution	10m	10m	3m
Downloaded year	2024	2024	2022

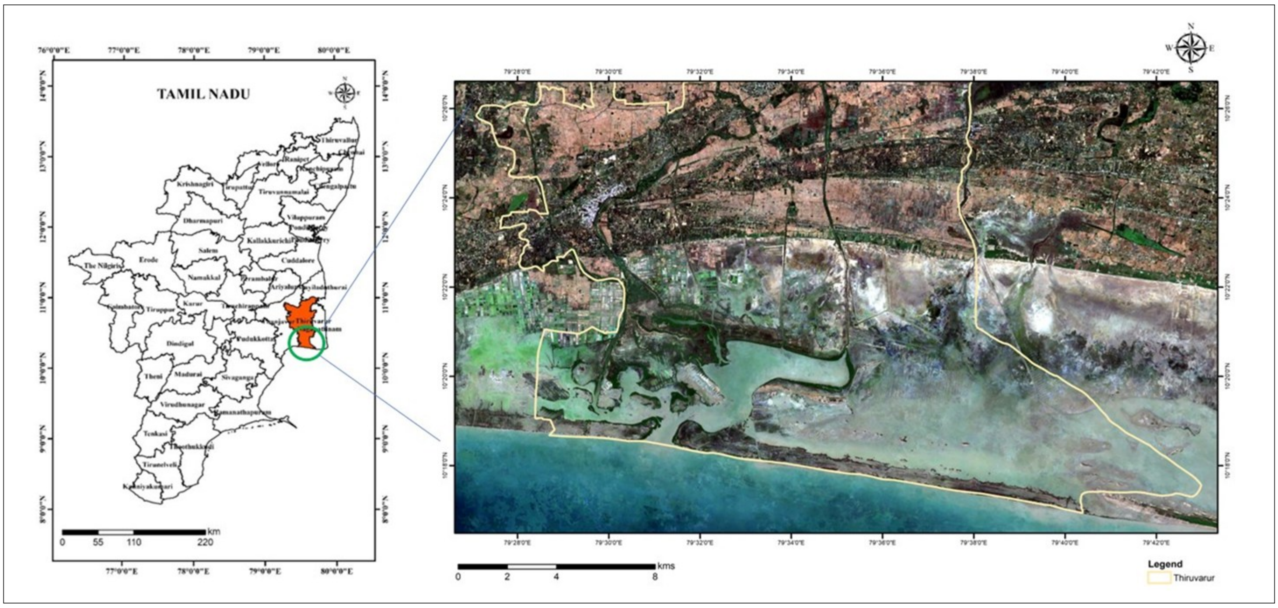

Fig. 1. Map of study area.

Sentinel-2 is a multispectral level 2A orthorectified and atmospherically corrected surface reflectance data with 10 m resolution. Temporal median reduction is applied to all images of Muthupet mangroves throughout 2024 with a cloud cover of less than 20 %.

Sentinel-1A is a C-band SAR data collection that provides calibrated and orthorectified data. All the preprocessing steps for Sentinel-1 SAR data are done in GEE and again the temporal median filter is applied for all images available throughout the year 2024. The images are reprojected to Sentinel-2 images.

Cloud-free high-resolution Planet Scope image downloaded for May 2022 to avoid the cloud cover, which is used for obtaining mangrove area points through visual interpretation. All the images are masked to our study area administrative boundary.

Mangrove classification using optical data

Optical vegetation indices used in this study

1. Normalized Difference Vegetation Index (NDVI) is widely used due to its simplicity and broad relevance but is less effective alone for detailed mangrove discrimination because of interference from water and wet soil backgrounds (19).
2. The Normalized Difference Water Index (NDWI) is widely used in mangrove studies primarily to estimate and discriminate water content and moisture levels, which are critical in distinguishing mangrove vegetation from open water and other land covers. NDWI is particularly valuable for delineating mangrove boundaries, given mangroves' characteristic coexistence with tidal waters (20).

Combined Mangrove Recognition Index (CMRI) is valid for assessing mangrove health and degradation by combining NDVI and NDWI, which are sensitive to vegetation and moisture but may be more complex and less broadly validated (21).

All the vegetation indices are calculated in the ArcMap environment using the raster calculator tool and the formulas for optical vegetation indices are given below in Table 2.

For the mangrove classification, a composite dataset was created by stacking all 13 spectral bands of Sentinel-2 imagery along with three vegetation indices: NDVI, NDWI and CMRI. The stacked dataset served as input for supervised classification using machine learning algorithms to delineate mangrove extents from other land cover types effectively. This integrated approach leverages the complementary strengths of multispectral bands and targeted vegetation indices to enhance classification accuracy and mapping reliability.

Table 2. Method and formula of NDVI, NDWI and CMRI (22)

Method	Formula
NDVI	(NIR-RED)/(NIR+RED)
NDWI	(NIR-SWIR)/(NIR+SWIR)
CMRI	(NIR-Red/NIR+Red) - (NIR-SWIR/NIR+SWIR)

Random forest classifier

Random forest is a supervised ensemble machine learning algorithm that constructs multiple decision trees during training and outputs the class that is the mode of the classes predicted by individual trees. It improves prediction accuracy and generalization by combining the results of these diverse trees using majority voting. This method effectively handles complex, high-dimensional data and reduces overfitting compared to single decision trees (23). Random forest has proven highly effective in discriminating between MFs and multispectral optical data, such as Sentinel-2 imagery. It efficiently utilizes numerous spectral bands and vegetation indices, capturing subtle spectral differences characteristic of mangroves (24). Mangrove environments are spectrally complex and often mixed with other vegetation types; Random forest handles this heterogeneity well without overfitting (25). Studies show that Random forest often outperforms methods such as Support Vector Machine (SVM) and Maximum Likelihood Classification (MLC), achieving overall accuracies greater than 95 %, with high precision and recall for mangrove classes (26,27). It can identify the most informative spectral bands and indices, helping optimize the classification model by focusing on key variables such as, visible and shortwave infrared bands along with vegetation indices (24).

Optical and SAR based mangrove index

This study used OSCMI mangrove extracting indices, which do not require tidal data and simply need a certain threshold to discriminate mangroves from other land cover types. Optical remote sensing images are often affected by clouds and fog, especially in tropical and subtropical regions, reducing their availability for mangrove mapping (28). Many mangrove indices require multi-temporal images of high tide and low tide to account for tidal flooding, which increases data demands and effort in data screening (14). Existing indices often perform well in specific areas with tall and dense mangroves but lack verification in regions with different mangrove types (e.g., short and sparse forests) (22,29). To address these issues in optical data a previous study developed new optical and SAR based mangrove index and the formula is as follows (10),

$$OSCMI = \frac{WI}{SWIRB + NIRB + VV}$$

Where VV is the backscatter coefficient of Sentinel-1 VV polarisation mode, NIRB is the sum of the reflectance of Sentinel-2 B6, B7, B8 and B8A, SWIRB is the sum of the reflectance of Sentinel-2 B11 and B12 and WI is the sum of NDWI and MNDWI (10). Green, NIR and SWIR1 are the reflectance for bands 3, 8 and 11, respectively for Sentinel-2.

When distinguishing mangrove from other vegetation, OSCMI and its sub-indices WI, NIRB and SWIRB were found to be more accurate than another optical mangrove index. These bands are identified by Statistical analysis of bands from Sentinel -1 SAR and Sentinel-2 optical images that effectively distinguish mangroves from other vegetation (10).

Accuracy assessment

Using Google Earth images and high-resolution Planet Scope images, the mangrove area was identified through visual interpretation. Totally two hundred and fifty mangrove sites and one hundred and fifty non-mangrove points were taken. The non -mangrove points include non-vegetation area and vegetation other than mangroves (Fig. 2). Out of these total one hundred and fifty mangrove points and one hundred non-mangrove points were used to train the classifier algorithm to classify mangrove area. The remaining hundred mangrove and fifty non-mangrove points were used for accuracy assessment for both OSCMI-based mangrove area and RF-based mangrove area.

Accuracy assessment for classified images is carried out through the confusion matrix and the kappa coefficient is used to evaluate the agreement between the images. The confusion matrix, also known as an error matrix, is a tabular representation that compares the predicted class labels from the classification process against the actual reference or ground truth data. Each row of the matrix represents the predicted class, while each column represents the reference class. This setup allows for the identification of correctly classified samples along the main diagonal and misclassifications off the diagonal.

The kappa coefficient provides a robust statistical measure of classification accuracy by accounting for the agreement that could occur by chance. Unlike overall accuracy, kappa adjusts for random agreements between classified and reference data, offering a more stringent assessment of classification performance. Values of kappa range from -1 to 1, where values closer to 1 indicate strong agreement beyond chance, values around 0 suggest random agreement and negative values signify less than chance agreement.

The combination of confusion matrix metrics and kappa coefficient enables a comprehensive and reliable accuracy assessment of the mangrove classification outcome, effectively quantifying classification performance and guiding improvements in classification methodology (30).

Result and Discussion

To distinguish mangroves from other land cover types, spectral indices including NDVI, NDWI and CMRI were extracted for three classes: Mangrove, Non-Vegetation and Other Vegetation for all training sites. The minimum and maximum values of each index across these classes are summarized below and interpreted to understand their spectral behavior and class separability (Table 2).

NDVI

NDVI values ranged from 0.779 to 0.896 for mangrove areas, indicating a consistently high density of green biomass. Other vegetation exhibited a broader NDVI range from -0.189 to 0.762,

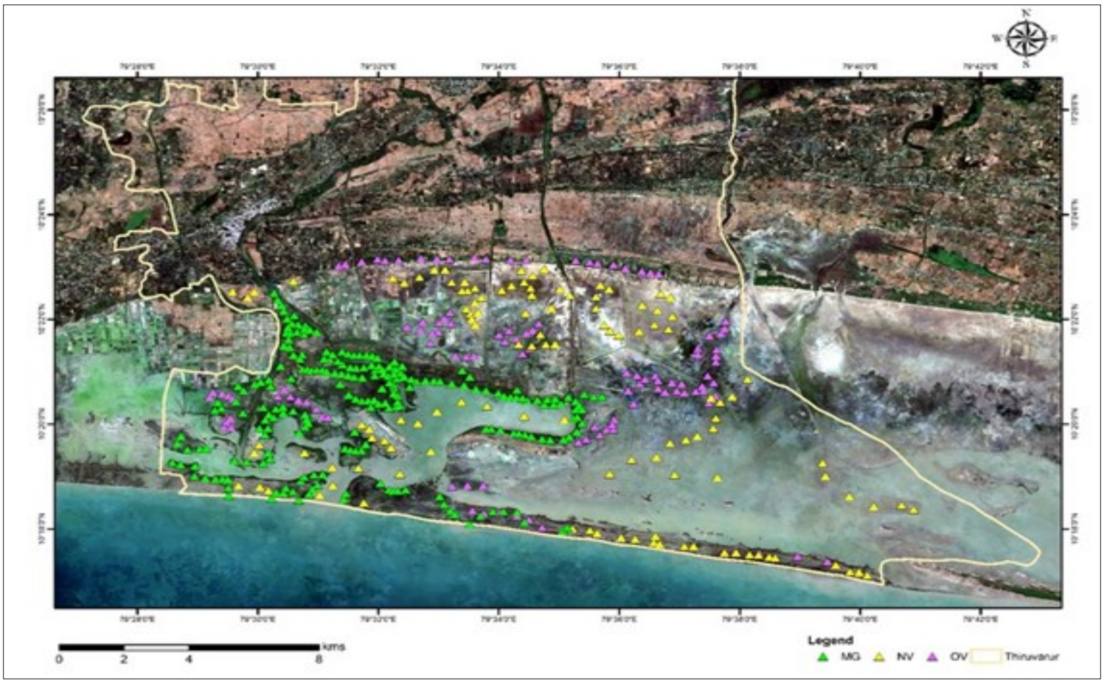

Fig. 2. Reference points collected for mangrove (MG), non-mangroves (NV) and other vegetation (OV).

reflecting a wider variability in vegetation cover and health. Non-vegetation areas showed NDVI values between -0.650 and 0.434, typical of barren land, built-up areas or water surfaces, which exhibit little to no vegetation reflectance. These results highlight NDVI's efficacy in discriminating dense vegetation (e.g., mangroves) from non-vegetated and sparsely vegetated areas. These results are consistent with previous studies**,** which reported that NDVI values for healthy mangrove stands typically exceed 0.7, making it a robust indicator for identifying dense mangrove cover globally (31). Landsat-derived NDVI utilized to map mangrove changes in the Sundarbans and found that NDVI values above 0.75 were closely correlated with high biomass mangrove patches (32). However, NDVI's effectiveness decreases in distinguishing mangroves from other forms of dense vegetation, as the maximum NDVI for other vegetation in this study was also relatively high (0.762). This overlap has been noted in a study which argued that while NDVI is useful for general vegetation mapping, its limitations in wetland ecosystems stem from spectral similarities among dense plant communities (33).

NDWI

Mangrove zones recorded NDWI values between -0.759 and -0.589, indicating moderate to low surface water presence beneath or surrounding vegetation canopies. Other vegetation showed NDWI values ranging from -0.655 to 0.161, suggesting the inclusion of both dryland vegetation and moisture-rich areas. Non-vegetation classes exhibited the widest NDWI range, from -0.424 to 0.761, which may be attributed to the presence of open water bodies and impervious surfaces. These findings suggest that NDWI alone may not be sufficient to isolate mangroves distinctly, but it can be helpful in conjunction with other indices. This aligns with previous that improved NDWI to enhance water body extraction and found that NDWI can vary significantly in mangrove zones due to tidal cycles and sub-canopy water masking (34). While NDWI aids in detecting water-rich environments, its application in mangrove mapping is context-dependent. NDWI may be less reliable for mature mangrove stands due to limited water signal from the canopy, which corroborates the modest NDWI values observed for mangroves in this study (35) .

CMRI

The CMRI provided a more integrated approach to identifying mangroves by combining vegetation and water index components. Mangrove regions exhibited CMRI values ranging from -0.759 to 0.896, reflecting the mixed spectral nature of these ecosystems, which are characterized by both vegetation and tidal influence. Other vegetation ranged from -0.655 to 0.762, while non-vegetation varied from -0.651 to 0.761. Although there is some overlap, mangroves exhibited higher maximum CMRI values, supporting their potential for enhanced mangrove detection compared to NDVI or NDWI alone. This is in agreement a previous study which proposed CMRI as a specialized index that integrates NDVI and NDWI to better isolate mangroves, particularly in regions with heterogeneous land cover (36). Furthermore, another study has highlighted the importance of integrating spectral indices for mangrove classification, suggesting that hybrid indices like CMRI improve accuracy in mixed environments compared to single-variable approaches (37).

Mangrove area and accuracy assessment

Box plots of various indices for the sampling sites is shown in Fig. 3. The mangrove area map for the study area was derived from optical imagery and OSCMI index-based threshold segmentation is depicted in Fig. 4 & 5. The OSCMI values for three classes are given in the Table 3. For mangrove areas, OSCMI values ranged from -0.821 to -0.492, indicating relatively lower index values due to the strong backscatter from dense vegetation and the presence of water beneath the canopy but this threshold ranges contrast with a previous work where the ranges are 0.04 to 0.07 (10). This discrepancy may be due to radiometric resolution of the satellite data and local ecological conditions including canopy density, water salinity, sediment content and background reflectance. In non-vegetation areas, values ranged from -0.692 to 8.540, with the wide upper range likely influenced by highly reflective surfaces such as bare soil, built-up areas, or mixed land types that contribute to elevated index responses. Other vegetation types showed OSCMI values between 1.011 and 1.648, representing higher reflectance from dry or upland vegetation with less water interaction and minimal radar backscatter.

Random forest classified mangrove area in Thiruvarur was estimated to be 1752 ha and OSCMI-based mangrove area was estimated to be 2027 ha. Based on a previous report, the total mangrove area of Thiruvarur district was 2142 ha where the OSCMI-based mangrove area estimation is 2027 ha, which has an agreement percentage of 94.63 (38). The accuracy assessment for the mangrove area was conducted using sampling points collected for mangrove and non-mangrove area. The confusion matrix for the Random forest classifier and the OSCMI classification area is given in Table 4 & 5.

The Random forest classifier achieved an overall accuracy of 84.7 % with a kappa coefficient of 0.66, indicating a moderate level of agreement between the classification and reference data. Although RF demonstrated a relatively high user's accuracy for mangroves (90.5 %), it underperformed in accurately identifying non-mangrove areas (UA = 74.5 %). The lower performance in mixed land-cover environments suggests that Random forest, while robust, may be challenged by spectral confusion in optical data for mangrove landscapes, as also reported by (33,39). The misclassification of mangroves by

Table 3. Summary of NDVI, NDWI and CMRI values for reference points

		Mangrove	Non-Vegetation	Other vegetation
NDVI	Min	0.779	-0.650	-0.189
	Max	0.895	0.434	0.762
NDWI	Min	-0.758	-0.423	-0.655
	Max	-0.589	0.760	0.160
CMRI	Min	-0.758	-0.650	-0.655
	Max	0.895	0.760	0.762
OSCMI	Min	-0.821	-0.692	1.011
	Max	-0.492	8.540	1.648

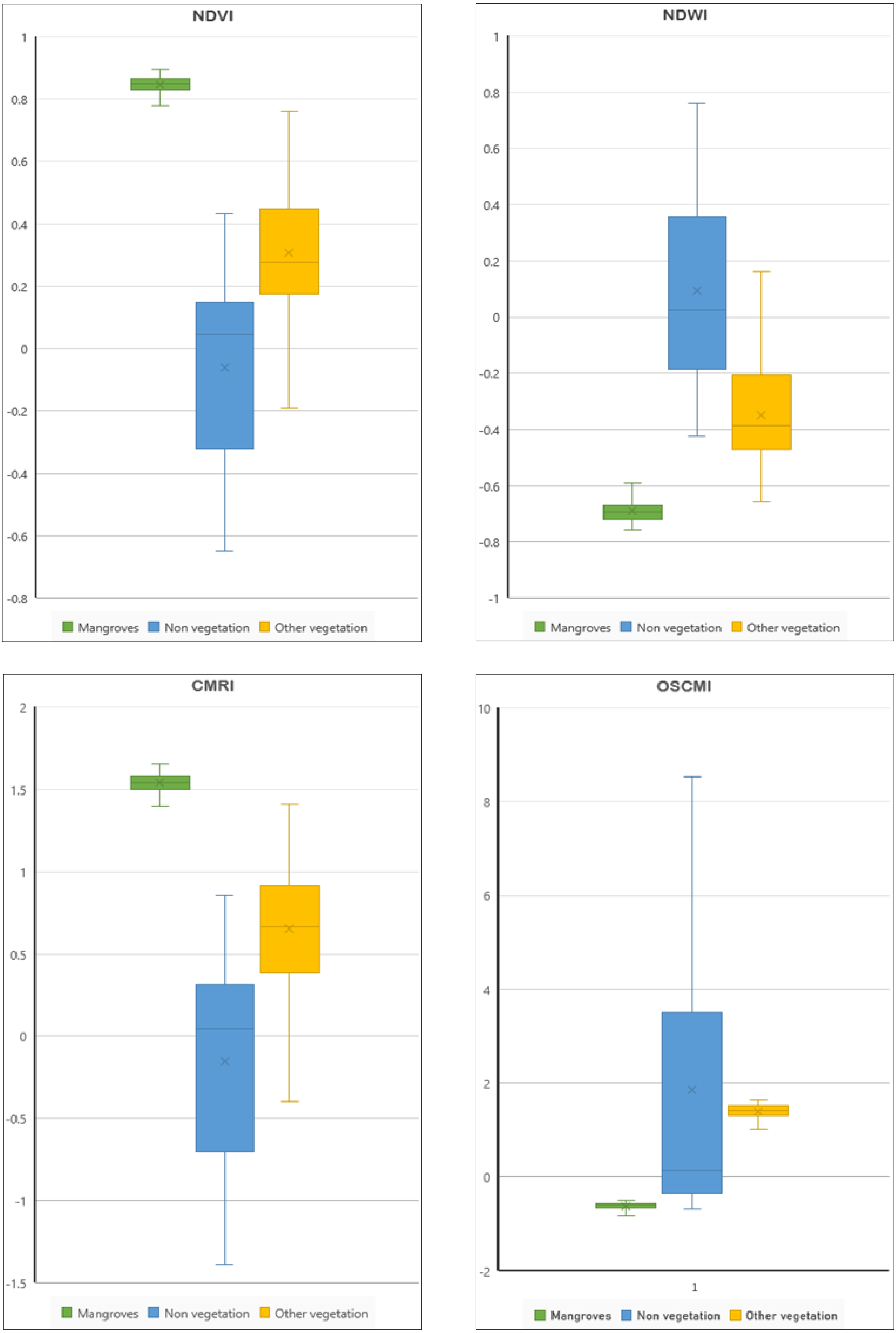

Fig. 3. Box plots of various indices for the sampling sites.

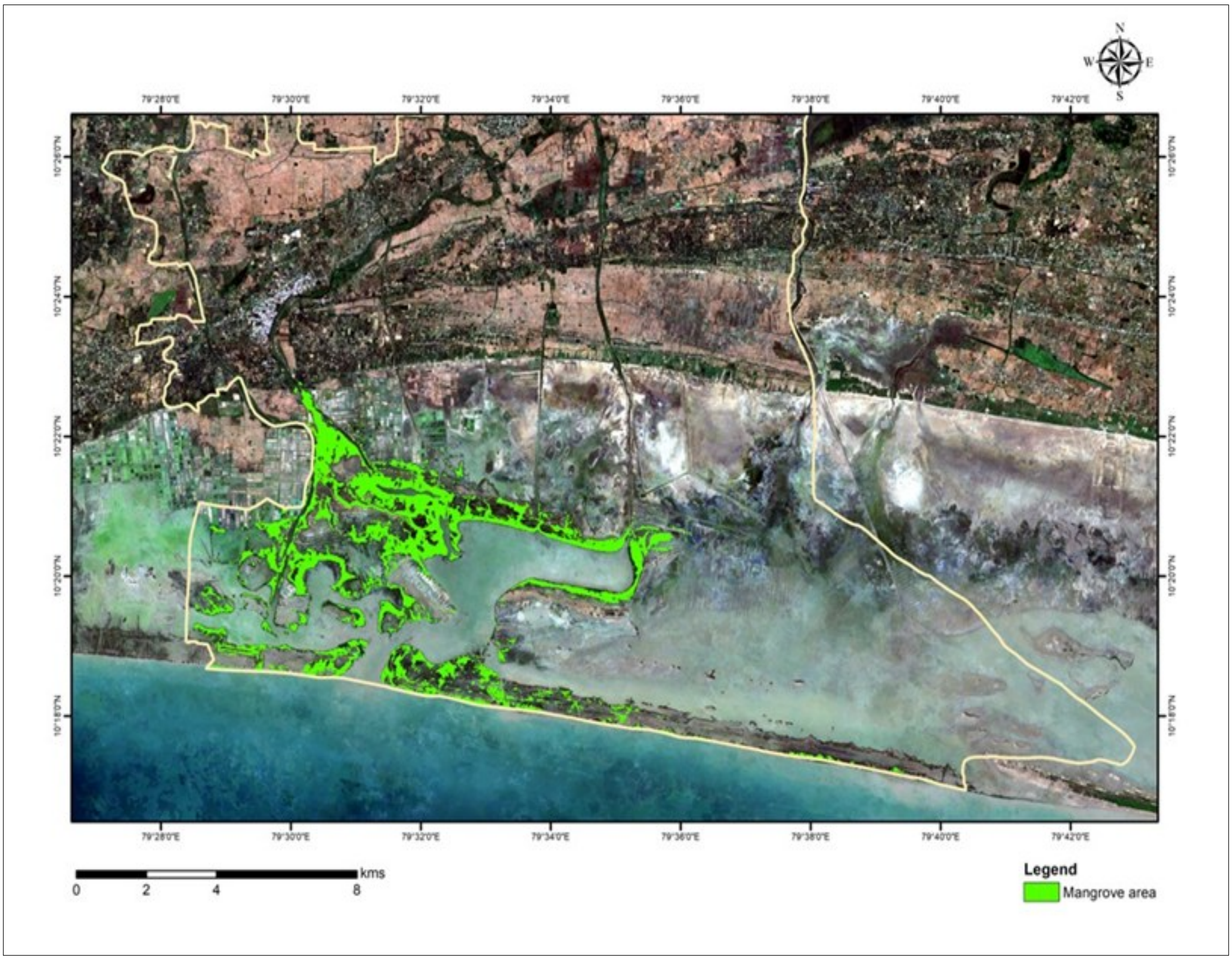

Fig. 4. Optical image-based mangrove area map using random forest classifier.

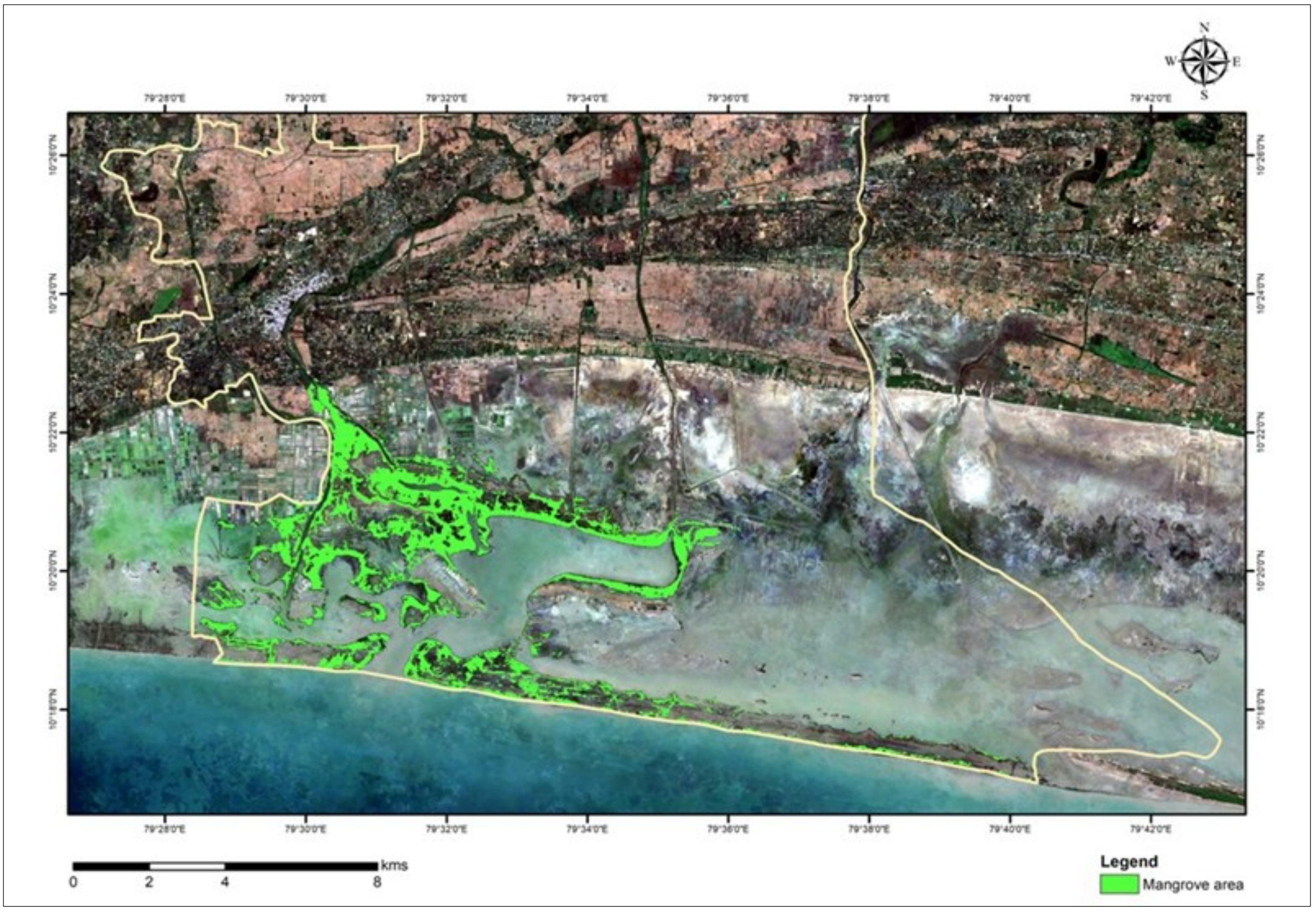

Fig. 5. OSCMI-based mangrove area map.

Table 4. Confusion matrix for random forest classification

	Mangrove	Non mangrove	PA
Mangrove	86	14	86.0 %
Non mangrove	9	41	82.0 %
UA	90.5 %	74.5 %	84.7 %
		Overall accuracy	84.7 %
		Kappa coefficient	0.66

Table 5. Confusion matrix for OSCMI classification

	Mangrove	Non mangrove	PA
Mangrove	92	8	92.0 %
Non mangrove	6	44	88.0 %
UA	93.9 %	84.6 %	90.7 %
		Overall accuracy	90.7 %
		Kappa coefficient	0.79

Random forest is due to limited training data, spectral similarities and complex land cover dynamics. In contrast, the OSCMI-based method exhibited a significantly higher overall accuracy of 90.7 % and a kappa coefficient of 0.79, indicating substantial agreement. Both the user's and producer's accuracy were consistently higher for mangrove and non-mangrove classes, showing improved classification reliability. This enhancement aligns with findings from (10,40) who introduced the use of OSCMI (a composite spectral index) for mangrove discrimination and demonstrated that it outperforms traditional classifiers in coastal wetland environments. The misclassification by OSCMI is due to the overlapping of index values and site-specific actors such as sedimentation, water salinity and spectral similarities (40).

OSCMI versus random forest

OSCMI is considered more effective than Random Forest (RF) classification using only optical imagery due to several key advantages:

Achieves higher accuracy

Previous studies demonstrated OSCMI has superior performance with overall accuracies reaching up to 96 %, which is generally higher than RF-based classifications with optical imagery, especially in areas with cloud cover and fog (10).

Addresses cloud cover issues

By fusing SAR data with optical imagery, OSCMI effectively overcomes the limitations posed by clouds and fog that hamper optical-only methods, leading to more reliable and consistent mangrove detection (41).

Simplifies the process

Unlike RF, which is a machine learning approach requiring training data, parameter tuning and computational resources, OSCMI is a threshold segmentation-based index. It requires only specific threshold values, making it simpler, faster and less skill-dependent (40).

Requires less skill and processing power

Since OSCMI uses a straightforward formula to identify mangroves, it is accessible for practitioners with limited expertise in machine learning, unlike RF which involves model training and validation procedures (42).

Effectiveness of OSCMI in mangrove classification

OSCMI effectively integrates information from both optical and SAR imagery, enhancing the discrimination of mangroves from other land cover types. This fusion approach leverages the complementary strengths of spectral and radar data, enabling more robust classification across diverse mangrove structures and conditions.

OSCMI demonstrates high performance in areas with both tall, dense MFs and short, sparse mangrove stands, making it particularly suitable for large-scale and heterogeneous mangrove mapping. One of the key improvements in OSCMI is the incorporation of VV polarization mode from SAR data, which enhances the recognition of mangrove pixels by capturing unique volume scattering and backscatter properties typical of mangrove habitats. This significantly reduces the rate of misclassification with non-mangrove vegetation. OSCMI is composed of multiple sensitive sub-indices, each contributing distinct ecological information.

Water Index (WI)

Reflects surface water content and habitat background, which is critical in identifying the inundated conditions of mangrove ecosystems.

Near-Infrared Band Ratio (NIRB)

Highlights canopy water content, supporting the differentiation of mangroves from upland vegetation.

Short-Wave Infrared Band Ratio (SWIRB)

Emphasizes variations in canopy reflectance, aiding in the separation of mangroves from other vegetative cover.

VV Polarization (SAR)

Enhances the identification of mangroves by exploiting the volume scattering effects and structural characteristics of mangrove canopies.

This integrative design provides a comprehensive spectral and structural representation of mangrove characteristics, making OSCMI a powerful tool for accurate and scalable mangrove mapping (29).

Conclusion

This study compares RF classification using optical data with OSCMI for mangrove mapping. Results show that OSCMI delivers higher accuracy and consistency, as confirmed by confusion matrices, overall accuracy and kappa coefficient. By combining optical and SAR data, OSCMI improves the separation of mangroves from other vegetation. Its multi-feature fusion and integration of spectral and backscatter data make it more robust than RF, offering a reliable solution for large-scale mangrove monitoring in complex coastal areas.

Acknowledgements

We are grateful to Centre for Water & Geospatial Studies, TNAU, Coimbatore, for providing financial support during the entire research activities and in the preparation of manuscript. We immensely delighted to convey our deepest and heartfelt thanks to Dr. D Muthumanickam, Professor & Head, Department of Remote Sensing & GIS, TNAU, Dr. K P Ragunath, Associate Professor (SS&AC), Centre for Water & Geospatial Studies, TNAU and Dr. R Jagadeeswaran, Professor (SS&AC), Department of Remote Sensing & GIS, TNAU for their altruistic guidance, tireless help and writing assistance towards this work. Special thanks to Mr. C Harichandran for his contribution towards preparation and submission of this manuscript.

Authors' contributions

All the authors contributed equally to the conceptualisation of the work, interpretation, analysis, writing, reviewing and editing of the manuscript. All authors read and approved the final manuscript.

Compliance with ethical standards

Conflict of interest: Authors do not have any conflict of interest to declare.

Ethical issues: None

References

1. India. Forest Survey of India. India state of the forest report 2023. Dehradun: Ministry of Environment, Forest and Climate Change; 2023
2. India. Tamil Nadu Green Climate Company. Mangroves of Tamil Nadu: coastal green warriors. Chennai: Department of Environment, Climate Change and Forest, Government of Tamil Nadu; 2024
3. Ward RD, Friess DA, Day RH, Mackenzie RA. Impacts of climate change on mangrove ecosystems: a region by region overview. Ecosyst Health Sustain. 2016;2(4):e01211. https://doi.org/10.1002/ehs2.1211
4. Alongi DM. Global meta-analysis of mangrove primary production: implications for carbon cycling in mangrove and other coastal ecosystems. Forests. 2025;16(5):747. https://doi.org/10.3390/f16050747
5. Sun Y, Zhao D, Guo W, Gao Y, Su X, Wei B. A review on the application of remote sensing in mangrove ecosystem monitoring. Acta Ecol Sin. 2013;33(15):4523-38. https://doi.org/10.5846/stxb201205150715
6. Conchedda G, Durieux L, Mayaux P. Object-based monitoring of land cover changes in mangrove ecosystems of Senegal. In: Proceedings of the 2007 International Workshop on the Analysis of Multi-temporal Remote Sensing Images; 2007 Jul 18-20; Leuven, Belgium. Piscataway (NJ): IEEE; 2007. p. 1-6. https://doi.org/10.1109/MULTITEMP.2007.4293039
7. Hidayah Z. Application of remote sensing in mangrove studies: a literature review. Jurnal Kelautan Indones J Mar Sci Technol. 2010;3(1):48-53.
8. Salghuna N, Pillutla R. Mapping mangrove species using hyperspectral data: a case study of Pichavaram mangrove ecosystem, Tamil Nadu. Earth Syst Environ. 2017;1:1-12. https://doi.org/10.1007/s41748-017-0024-8
9. Ghorai D, Mahapatra M, Paul AK. Application of remote sensing and GIS techniques for decadal change detection of mangroves along Tamil Nadu coast, India. J Remote Sensing GIS. 2016;7(1):42-53.
10. Huang K, Yang G, Yuan Y, Sun W, Meng X, Ge Y. Optical and SAR images combined mangrove index based on multi-feature fusion. Sci Remote Sens. 2022;5:100040. https://doi.org/10.1016/j.srs.2022.100040
11. Xue J, Su B. Significant remote sensing vegetation indices: a review of developments and applications. J Sensors. 2017;2017(1):1353691. https://doi.org/10.1155/2017/1353691
12. Wang J, Xiao X, Bajgain R, Starks P, Steiner J, Doughty RB, et al. Estimating leaf area index and aboveground biomass of grazing pastures using Sentinel-1, Sentinel-2 and Landsat images. ISPRS J Photogramm Remote Sens. 2019;154:189-201. https://doi.org/10.1016/j.isprsjprs.2019.06.007
13. Zhao C, Qin CZ. 10-m-resolution mangrove maps of China derived from multi-source and multi-temporal satellite observations. ISPRS J Photogramm Remote Sens. 2020;169:389-405. https://doi.org/10.1016/j.isprsjprs.2020.10.001
14. Xia Q, Qin CZ, Li H, Huang C, Su FZ. Mapping mangrove forests based on multi-tidal high-resolution satellite imagery. Remote Sens. 2018;10(9):1343. https://doi.org/10.3390/rs10091343
15. Xia Q, Qin CZ, Li H, Huang C, Su FZ, Jia MM. Evaluation of submerged mangrove recognition index using multi-tidal remote sensing data. Ecol Indic. 2020;113:106196. https://doi.org/10.1016/j.ecolind.2020.106196
16. Zhang H, Wang T, Liu M, Jia M, Lin H, Chu L, et al. Potential of combining optical and dual polarimetric SAR data for improving mangrove species discrimination using rotation forest. Remote Sens. 2018;10(3):467. https://doi.org/10.3390/rs10030467
17. Selvaraj A, Saravanan S, Rani N. Development of spectral library of mangrove native species of the Muthupet lagoon, Tamil Nadu, India using field spectroscopic instrument. Indian J Geo-Mar Sci. 2020;49(5):809-15.
18. Amani M, Ghorbanian A, Ahmadi SA, Kakooei M, Moghimi A, Mirmazloumi SM, et al. Google Earth Engine cloud computing platform for remote sensing big data applications: a comprehensive review. IEEE J Sel Top Appl Earth Obs Remote Sens. 2020;13:5326-50. https://doi.org/10.1109/JSTARS.2020.3021052
19. Tran TV, Reef R, Zhu X. A review of spectral indices for mangrove remote sensing. Remote Sens. 2022;14(19):4868. https://doi.org/10.3390/rs14194868
20. Upakankaew K, Ninsawat S, Virdis SG, Sasaki N. Discrimination of mangrove stages using multitemporal Sentinel-1 C-band backscatter and Sentinel-2 data: a case study in Samut Songkhram Province, Thailand. Forests. 2022;13(9):1433. https://doi.org/10.3390/f13091433
21. Winarso G, Purwanto AD. Evaluation of mangrove damage level based on Landsat 8 image. Int J Remote Sens Earth Sci. 2017;11(2):105-16. https://doi.org/10.30536/j.ijreses.2014.v11.a2608
22. Gupta K, Mukhopadhyay A, Giri S, Chanda A, Majumdar SD, Samanta S, et al. An index for discrimination of mangroves from non-mangroves using Landsat 8 OLI imagery. MethodsX. 2018;5:1129-39. https://doi.org/10.1016/j.mex.2018.09.011
23. Cherian SM, Kanjirappuzha R. Random forest and support vector machine classifiers for coastal wetland characterization using the combination of features derived from optical data and synthetic aperture radar dataset. J Water Climate Change. 2024;15(1):29-49. https://doi.org/10.2166/wcc.2023.238
24. Shen Z, Miao J, Wang J, Zhao D, Tang A, Zhen J. Evaluating feature selection methods and machine learning algorithms for mapping mangrove forests using optical and synthetic aperture radar data. Remote Sens. 2023;15(23):5621. https://doi.org/10.3390/rs15235621
25. Jhonnerie R, Siregar VP, Nababan B. Comparison of random forest algorithm implemented on object and pixel based classification for mangrove land cover mapping. ICST. 2017;1:292-302.
26. Purwanto AD, Wikantika K, Deliar A, Darmawan S. Decision tree and random forest classification algorithms for mangrove forest mapping in Sembilang National Park, Indonesia. Remote Sens. 2022;15(1):16. https://doi.org/10.3390/rs15010016

27. Intarat K, Sillaparat S. Tropical mangrove species classification using random forest algorithm and very high-resolution satellite imagery. Burapha Sci J. 2019:742-53.

28. Fang X, Ying Z, Liang Z, Jia L, Xianghui G. Extraction method of intertidal mangrove by using Sentinel-2 images. Bull Surv Mapping. 2020(2):49.

29. Jia M, Wang Z, Wang C, Mao D, Zhang Y. A new vegetation index to detect periodically submerged mangrove forest using single-tide Sentinel-2 imagery. Remote Sens. 2019;11(17):2043. https://doi.org/10.3390/rs11172043

30. Amalo L, Setiawan Y, Kusmana C. Spatio-temporal dynamics of mangrove extent in coastal Bekasi Regency, Indonesia. In: IOP Conference Series: Earth and Environmental Science; 2023 Jul 10-12; Bekasi, Indonesia. Bristol: IOP Publishing; 2023. p. 012005. https://doi.org/10.1088/1755-1315/1266/1/012005

31. Giri C, Ochieng E, Tieszen LL, Zhu Z, Singh A, Loveland T, et al. Status and distribution of mangrove forests of the world using earth observation satellite data. Glob Ecol Biogeogr. 2011;20(1):154-9. https://doi.org/10.1111/j.1466-8238.2010.00584.x

32. Akbar M, Arisanto P, Sukimo B, Merdeka P, Priadhi M, Zallesa S. Mangrove vegetation health index analysis by implementing NDVI classification method on Sentinel-2 image data: case study Segara Anakan, Kabupaten Cilacap. In: IOP Conference Series: Earth and Environmental Science; 2020 Oct 14-16; Cilacap, Indonesia. Bristol: IOP Publishing; 2020. p. 012069. https://doi.org/10.1088/1755-1315/584/1/012069

33. Heumann BW. Satellite remote sensing of mangrove forests: recent advances and future opportunities. Prog Phys Geogr. 2011;35(1):87-108. https://doi.org/10.1177/0309133310385371

34. Xu H. Modification of normalised difference water index (NDWI) to enhance open water features in remotely sensed imagery. Int J Remote Sens. 2006;27(14):3025-33. https://doi.org/10.1080/01431160600589179

35. Lucas R, Van De Kerchove R, Otero V, Lagomasino D, Fatoyinbo L, Omar H, et al. Structural characterisation of mangrove forests achieved through combining multiple sources of remote sensing data. Remote Sens Environ. 2020;237:111543. https://doi.org/10.1016/j.rse.2019.111543

36. Singgalen YA, Manongga D. Monitoring of mangrove ecotourism area using NDVI, NDWI and CMRI in Dodola Island, Morotai Island Regency, Indonesia. J Ilmu Teknol Kelaut Tropis. 2022;14(1):95-108. https://doi.org/10.29244/jitkt.v14i1.37605

37. Kuenzer C, Bluemel A, Gebhardt S, Quoc TV, Dech S. Remote sensing of mangrove ecosystems: a review. Remote Sens. 2011;3(5):878-928. https://doi.org/10.3390/rs3050878

38. T.N.'s mangrove cover grows to 9,039 ha in 2024, has significant carbon stock: report. The Hindu. 2025 Mar 16 https://tinyurl.com/3pucp6v7

39. Dronova I. Object-based image analysis in wetland research: a review. Remote Sens. 2015;7(5):6380-413. https://doi.org/10.3390/rs70506380

40. Zablan C, Blanco A, Nadaoka K, Martinez K, Baloloy A. Assessment of mangrove extent extraction accuracy of threshold segmentation-based indices using Sentinel imagery. Int Arch Photogramm Remote Sens Spatial Inf Sci. 2023;48:391-401. https://doi.org/10.5194/isprs-archives-XLVIII-4-W6-2022-391-2023

41. Xu Z, Chen KS. On signal modeling of moon-based synthetic aperture radar imaging of earth. Remote Sens. 2018;10(3):486. https://doi.org/10.3390/rs10030486

42. Belgiu M, Dragut L. Random forest in remote sensing: a review of applications and future directions. ISPRS J Photogramm Remote Sens. 2016;114:24-31. https://doi.org/10.1016/j.isprsjprs.2016.01.011

Additional information

Peer review: Publisher thanks Sectional Editor and the other anonymous reviewers for their contribution to the peer review of this work.

Reprints & permissions information is available at https://horizonepublishing.com/journals/index.php/PST/open_access_policy

Publisher's Note: Horizon e-Publishing Group remains neutral with regard to jurisdictional claims in published maps and institutional affiliations.

Indexing: Plant Science Today, published by Horizon e-Publishing Group, is covered by Scopus, Web of Science, BIOSIS Previews, Clarivate Analytics, NAAS, UGC Care, etc
See https://horizonepublishing.com/journals/index.php/PST/indexing_abstracting

Publisher information: Plant Science Today is published by HORIZON e-Publishing Group with support from Empirion Publishers Private Limited, Thiruvananthapuram, India.